Gene Therapy (2015) **22,** 127–137

www.nature.com/gt

ORIGINAL ARTICLE

Inhibition of choroidal fibrovascular membrane formation by new class of RNA interference therapeutic agent targeting periostin

T Nakama[1], S Yoshida[1], K Ishikawa[1], Y Kobayashi[1], Y Zhou[1], S Nakao[1], Y Sassa[1,2], Y Oshima[1], K Takao[3], A Shimahara[3], K Yoshikawa[3], T Hamasaki[4], T Ohgi[4], H Hayashi[4], A Matsuda[5], A Kudo[6], M Nozaki[7], Y Ogura[7], M Kuroda[8] and T Ishibashi[1]

Age-related macular degeneration (AMD) is a vision-threatening disease characterized by choroidal fibrovascular membrane (FVM) formation, choroidal neovascularization (CNV) and choroidal fibrosis. No safe and effective therapeutic method has been developed for the choroidal fibrosis, although anti-vascular endothelial growth factor therapy can partially shrink the CNV. We recently reported that periostin (POSTN), which is produced by retinal pigment epithelial cells, has an important role in the formation of preretinal FVMs, but its role in choroidal FVMs has not been determined. In this study, we used *Postn* knockout mice to investigate the role played by POSTN in choroidal FVM formation. In addition, we used a new class of RNA interference (RNAi) agent (NK0144) that targets POSTN and determined its effect on choroidal FVM development. Genetic ablation of *Postn* had an inhibitory effect not only on CNV formation but also on choroidal fibrosis in a mouse CNV model. NK0144 also had a greater inhibitory effect on both the CNV and choroidal fibrosis than control RNAi with no apparent adverse effects. These findings suggest a causal relationship between POSTN and choroidal FVM formation, and also a potential therapeutic role of intravitreal NK0144 for AMD.

Gene Therapy (2015) **22,** 127–137; doi:10.1038/gt.2014.112; published online 11 December 2014

INTRODUCTION

Age-related macular degeneration (AMD) is a leading cause of a severe reduction of vision in the elderly population of developed countries.[1–3] It is estimated that the prevalence of AMD will increase, which would then increase both the social and medical burdens of the countries. At the advanced stage of AMD, choroidal fibrovascular membranes (FVMs), which consist of choroidal neovascularization (CNV) and choroidal fibrosis form, and they can lead to severe vision reduction.[4–6] In this process, there is proliferation, adhesion and migration of various types of cells, for example, vascular endothelial cells, retinal pigment epithelial (RPE) cells, glial cells, fibroblasts and macrophages/monocytes. There is also deposition of extracelluar matrices.[7–10] Several growth factors, such as vascular endothelial growth factors (VEGFs), placental growth factor, connective tissue growth factor and transforming growth factor βs (TGF-βs) and their receptors, are involved in this process.[6,11–13] Among these, the VEGFs have been well characterized and are known to have a critical role in CNV formation. Anti-VEGF therapies have been proven to inhibit the progression of CNVs to some degree, but the different types of therapies have not been able to inhibit choroidal fibrosis.[14] In addition, it was recently reported that the intravitreal injection of anti-VEGF antibodies can cause retinal damage and promote choroidal fibrosis.[8,14–16] Therefore, choroidal FVM formation, especially choroidal fibrosis, remains a severe vision-threatening pathological condition.

We have recently demonstrated that there was an increase in the expression of periostin (POSTN) in the vitreous and FVMs of patients with proliferative diabetic retinopathy and proliferative vitreoretinopathy.[17–20] POSTN, a 90-kDa secreted matricellular protein, is a member of the fasciclin (fas) family. It is composed of an amino-terminal EMI domain, tandem repeat of four fas I domains and a carboxyl-terminal domain including a heparin-binding site at its C-terminal end.[21] POSTN interacts directly with the extracelluar matrices, including fibronectin, tenascin c and collagen type I, through its EMI and fas I domains. Furthermore, POSTN also serves as a ligand for integrins, such as $\alpha_v\beta_3$ and $\alpha_v\beta_5$. Through these interactions, POSTN is associated with the development and remodeling of tissues.[22] Recent studies have shown that POSTN promotes a regeneration of heart tissue after myocardial infarction, cutaneous wound healing and chronic allergic inflammation.[23–28] These findings indicate that POSTN has fundamental roles in tissue repair in several organs, and thus raises the possibility that POSTN may also be involved in the development of choroidal FVMs.

RNA interference (RNAi) is a natural mechanism of post-transcriptional silencing of gene expression that has been recently considered to be a new type of therapeutic system.[29] As a result of their high selectivity and potency, RNAi-based therapy has several advantages over conventional therapeutic approaches such as antibody, aptamer and antisense therapy. In addition, RNAi agents can be easily synthesized and the steps that are necessary

[1]Department of Ophthalmology, Kyushu University Graduate School of Medical Sciences, Fukuoka, Japan; [2]Department of Ophthalmology, Fukuoka University Chikushi Hospital, Fukuoka, Japan; [3]AQUA Therapeutics Co., Ltd., Kobe, Japan; [4]Strategic Headquarters for Research and Development, BONAC Corporation, BIO Factory, Fukuoka, Japan; [5]Department of Ophthalmology, Juntendo University School of Medicine, Tokyo, Japan; [6]Department of Biological Information, Tokyo Institute of Technology, Yokohama, Japan; [7]Department of Ophthalmology and Visual Science, Nagoya City University Graduate School of Medical Sciences, Nagoya, Japan and [8]Department of Molecular Pathology, Tokyo Medical University, Tokyo, Japan. Correspondence: Dr S Yoshida, Department of Ophthalmology, Kyushu University Graduate School of Medical Sciences, Fukuoka, 812-8582, Japan.
E-mail: yosida@eye.med.kyushu-u.ac.jp
Received 13 May 2014; revised 23 September 2014; accepted 24 October 2014; published online 11 December 2014

to identify and optimize them are rapid. However, previous investigations using canonical double-stranded small interfering RNAs (siRNAs) showed several obstacles including the lack of a safe drug delivery system (DDS), adverse off-target effects through Toll-like receptor 3 (TLR3) activation, and the lack of stability.[30–34]

In this study, we used a new class of single-stranded RNAi therapeutic agent, which can overcome those obstacles.[35] In addition, it is expected that the cost of large-scale production of single-stranded RNAi can be reduced because of the simple synthesizing method.

Based on these reports including ours, we hypothesized that POSTN is involved in choroidal FVM formation and can be used as a therapeutic target. To test this, we determined the expression and function of POSTN in human FVM specimens and in a mouse CNV model. We also studied the inhibitory effect of a new class of single-stranded RNAi agent targeting POSTN on choroidal FVM formation.

RESULTS

Expression of POSTN in RPE cells of choroidal FVMs in CNV mouse model and AMD patients

To determine whether POSTN is involved in the development of choroidal FVMs, real-time reverse transcription-PCR (RT-PCR) was performed and the expression of the mRNA of *Postn* in the RPE-choroid complexes after laser injury were compared with that in normal RPE-choroid complexes. The expression of *Postn* mRNA in a mouse CNV model group was significantly upregulated compared with the control group and reached a peak on day 14 ($P < 0.05$, $n = 4$; Figure 1a).

To confirm the result of real-time RT-PCR, we performed enzyme-linked immunosorbent assay (ELISA) to determine the concentration of the protein of POSTN. ELISA showed that the level of POSTN protein in the RPE-choroid complexes of CNV model mice was significantly higher from day 3 (75.41 ± 10.95 pg POSTN per mg total protein, $P < 0.05$; $n = 4$) than that in the control group (31.97 ± 0.65 pg POSTN per mg total protein; $n = 4$). The concentration reached a peak on day 14 (125.18 ± 16.76 pg POSTN per mg total protein, $P < 0.001$; $n = 4$; Figure 1b).

Next, sections were stained with antibodies to determine the localization of the POSTN in the choroidal FVMs. Immunohistochemical analyses showed POSTN-positive staining in RPE65-positive RPE cells after the laser injury (Figure 2a). In the human choroidal FVMs, POSTN stained the cytokeratin-positive RPE cells (Figure 2b). These findings indicated that the expression of the POSTN was increased in the RPE cells in both mouse CNV model and in the FVMs of AMD patients.

Choroidal FVM formation is reduced in *Postn* KO mouse

To investigate whether POSTN enhances the development of choroidal FVMs, we quantified the volume of the CNVs at day 7 and fibrous volumes at day 21 in both wild-type (WT) and *Postn* knockout (KO) mice. The average CNV volumes stained by isolectin B4 was $63\,400 \pm 2891\ \mu m^3$ in the *Postn* KO mice group ($n = 6$), which was significantly smaller by 34% than that of WT mice group at $96\,222 \pm 311\ \mu m^3$ ($P < 0.01$, $n = 6$; Figures 3a and b). There was a 59% reduction in average fibrosis volume (stained by collagen type I antibody) in *Postn* KO mice group at $21\,166 \pm 2886\ \mu m^3$ ($n = 6$) than in the WT mice at $51\,332 \pm 5665\ \mu m^3$ ($P < 0.05$, $n = 6$; Figures 3a and b).

NK0144-mediated inhibition of *POSTN* mRNA in cultured human RPE cells

Four types of RNAi agents including controls were synthesized as described in the Materials and methods section. A summary of RNAi agents were shown in Table 1, and the structure of RNAi agents were shown in Figure 4 (Figures 4a and b). The synthesized targeted sequence of RNAi agents for POSTN is present in not only human POSTN but also in mouse, rat, rabbit and rhesus macaque POSTN. This indicates that the direct animal testing of NK0144 would also be suitable for human clinical trials.

To determine if transfection with NK0144 inhibited the expression of the mRNA of *POSTN*, cell culture studies of human RPE cells, which are the cellular source of POSTN and important cells for ocular fibrosis, were carried out. Real-time RT-PCR showed that the levels of *POSTN* mRNA were significantly decreased following exposure of ARPE19 cells to 0.01, 0.1 and 1 nM of NK0144 in a dose-dependent manner, and almost completely blocked the expression of the mRNA of *POSTN* following exposure to 1 nM NK0144 ($P < 0.0001$, $n = 4$; Figure 4c). In contrast, the expression was not inhibited after exposure to 0.01, 0.1 and 1 nM of NI0000 as the negative control siRNA.

To determine whether transfection by NK0144 was cytotoxic, we performed cell viability assays. No significant difference in cell viability was observed at 24, 48 and 72 h after transfection between human primary RPE cells with 10 nM NK0144 transfection and those with control siRNA transfection ($n = 4$; Figure 4d).

Inhibitory effect of NK0144 on proliferation, adhesion and migration of human RPE cells *in vitro*

Next, we examined the effect of NK0144 on the proliferation, adhesion and migration of human RPE cells because these biological processes are involved in FVM formation, and they are facilitated by POSTN.[20] The proliferation of RPE cells was significantly inhibited by 10 nM NK0144 transfection ($P < 0.01$, $n = 4$; Figure 5a) as was cell adhesion ($P < 0.001$, $n = 4$; Figure 5b).

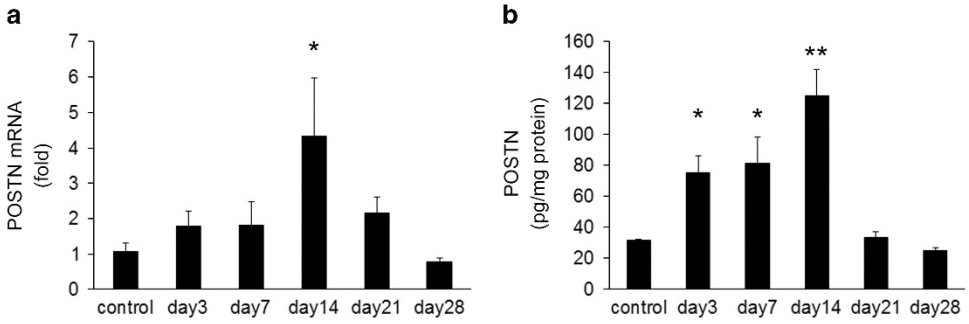

Figure 1. Expression of the mRNA of *POSTN* determined by real-time RT-PCR (**a**) and the concentration of POSTN protein measured by ELISA (**b**) in mouse eyes with laser-induced CNV. Bruch's membrane was ruptured at 20 locations in each eye. On days 3, 7, 14, 21 and 28 after the laser photocoagulations, mice were killed, eyes were removed, and both the total RNA and protein were extracted from the RPE-choroidal complexes. The POSTN expression was significantly increased and reached a peak at 14 days after the laser photocoagulation ($n = 4$ per group). $^*P < 0.05$, $^{**}P < 0.001$ vs control.

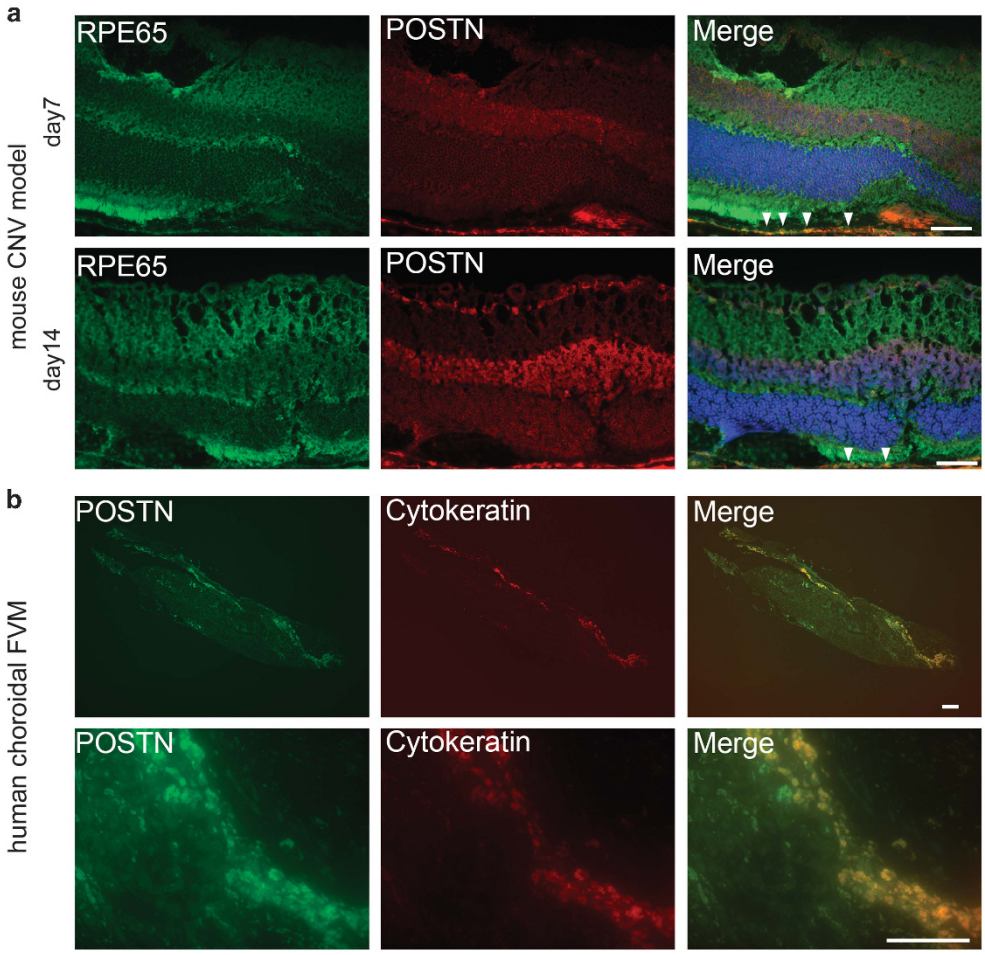

Figure 2. Localization of POSTN in laser-induced CNV in a mouse model (**a**) and human choroidal FVMs (**b**). Paraffin-embedded sections of eyes from the CNV mouse model and human choroidal FVMs resected during vitrectomy were immunohistochemically stained for POSTN, RPE65 and cytokeratin. Nuclei were stained with DAPI. These sections were examined by fluorescence microscopy. (**a**) POSTN (red) costained with RPE65 (green) in the choroidal FVM of CNV mice both at day 7 (top row) and day 14 (bottom row) when the expression of POSTN in RPE-choroid complexes is maximal. Scale bars = 50 μm. (**b**) Double staining for POSTN and cytokeratin in the human choroidal FVM. POSTN (green) staining in cytokeratin-positive RPE cells can be seen. A POSTN-stained section in the top panel is shown at higher magnification at the bottom. Scale bars = 200 μm.

In addition, the inhibitory effect of NK0144 on cell adhesion was by approximately 40%, which was significantly greater than after NI0079 transfection ($P < 0.01$, $n = 4$; Figure 5b). Finally, the migration of RPE cells was significantly impaired by NK0144 transfection ($P < 0.01$, $n = 4$; Figure 5c).

In situ distribution of fluorescein isothiocyanate (FITC)-labeled NK0144 in eyes after intravitreal injection

To determine the distribution and kinetics of NK0144 after intravitreal injection in mouse eyes, we used FITC-labeled NK0144. Twenty-four hours after the intravitreal injection of 1 μl of 100 μM FITC-labeled NK0144, there was staining for FITC in the RPE cells adjacent to the CNV site (Figure 6a). The degree of staining was increased at 72 h and then decreased at 120 h although it was still detectable (Figure 6a). These results showed that NK0144 rapidly diffused to the RPE cells around the CNV sites after the intravitreal injection and remained in that area for several days after the injection.

In vivo inhibitory effect of NK0144 on expression of *Postn* mRNA and progression of choroidal FVM formation

To determine whether NK0144 also causes a specific knock-down of *Postn in vivo* and has therapeutic potential, it was injected intravitreally in the CNV mouse model. Laser-capture microdissection was used to extract pure mRNA from the CNV sites (Figure 6b). On day 14 at the peak of *Postn* expression, the level of *Postn* mRNA in CNV site was significantly decreased after the intravitreal injection of 10 μM of NK0144, whereas there was no significant difference between NK0000 injection group and phosphate-buffered saline (PBS) injection group (Figure 6c).

At 7 days after rupturing Bruch's membrane, eyes that received an intravitreal injection of 1 μl of 10 μM NK0000 as a negative control developed larger areas of CNV than eyes after 1 μl of 10 μM NK0144 injections (Figure 7a). Compared with the control NK0000-treated eyes, the volume of the CNV in eyes treated with NK0144 was reduced by 75% ($P < 0.05$, $n = 8$; Figure 7b).

We further investigated the effect of NK0144 on choroidal fibrosis. At day 21, the volume of the choroidal fibrous tissues in eyes treated with 1 μl of 10 μM NK0144 was 30% smaller than that treated with NK0000 as a negative control ($P < 0.05$, $n = 8$; Figures 7a and b). These results are consistent with those of *Postn* KO mice (Figure 3).

No off-target effect on TLR3 activation by NK0144 in CNV development

As earlier reports showed that naked canonical double-stranded siRNA can suppress CNV formation not by RNAi but by target

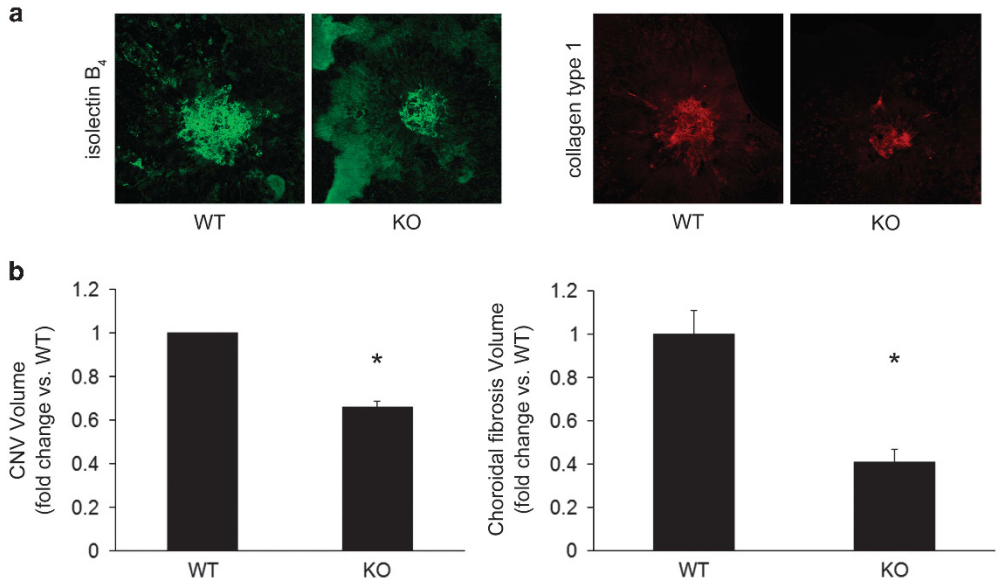

Figure 3. The mean volume of the CNV at day 7 and choroidal fibrosis at day 21 in laser-induced CNV mouse model. WT and *Postn* KO mice had laser photocoagulation (4–6 shots per eye) on day 0. The choroidal flat mounts were stained with isolectin B4 and collagen type I and were examined by laser scanning confocal microscopy. The volumes of the CNV on day 7 and choroidal fibrous tissue on day 21 at the laser sites were measured. (**a**) Representative immunohistochemical studies showing that the areas of CNV and choroidal fibrosis are smaller in *Postn* KO mice than in WT mice. (**b**) Both CNV and choroidal fibrosis volumes in *Postn* KO mice were significantly smaller than those in WT mice ($n = 6$ per group). $^*P < 0.05$.

Table 1. Sequence of RNAi agents directed against POSTN mRNA

Name	*RNA class*	*Sequence*
NI0079	Canonical double-stranded target siRNA	5′-GCACCAAAAAGAAAUACUUTT-3′ (sense)/5′-AAGUAUUUCUUUUUGGUGCTT-3′ (antisense)
NI0000	Canonical double-stranded scrambled siRNA	5′-UACUAUUCGACACGCGAAGTT-3′ (sense)/5′-CUUCGCGUGUCGAAUAGUATT-3′ (antisense)
NK0144	New class single-stranded target RNAi agent	5′-AGCACCAAAAAGAAAUACUUUUCCCCACACCGGA AAAGUAUUUCUUUUUGGUGCUUCUUCGG-3′
NK0000	New class single-stranded scrambled RNAi agent	5′-AUACUAUUCGACACGCGAAGUUCCCCACACCG GAACUUCGCGUGUCGAAUAGUAUUCUUCGG-3′

Abbreviations: POSTN, periostin; RNAi, RNA interference; siRNA, small interfering RNA.

sequence-independent activation of cell surface TLR3,[31,33] we examined the effect of a new class of RNAi agents, NK0000 and NK0144, on TLR3 phosphorylation in RPE cells *in vitro* by western blot. TLR3 phosphorylation was not increased 30 min after transfection with NK0000 or NK0144, whereas transfection with canonical siRNAs, NI0000 and NI0079, promoted TLR3 phosphorylation (Figure 8a). To further confirm the absence of off-target effects by the new class of RNAi, we performed ELISA of interleukin-12 (IL-12), which is a downstream signaling marker of TLR3 activation.[31] There was no significant difference between the level of IL-12 protein in the supernatant from RPE cells transfected with NK0000 or NK0144 (NK0000; 168.42 ± 26.08 pg IL-12 per mg total protein, NK0144; 140.86 ± 11.36 pg IL-12 per mg total protein; $n = 4$) and that from RPE cells without transfection (129.50 ± 23.02 pg IL-12 per mg total protein; $n = 4$). In contrast, the IL-12 level from RPE cells transfected with NI0000 or NI0079 were significantly higher (NI0000; 243.25 ± 38.06 pg IL-12 per mg total protein, NI0079; 300.48 ± 71.24 pg IL-12 per mg total protein, $P < 0.05$; $n = 4$) compared with the normal control (Figure 8b).

We also performed ELISA of interferon gamma, which is another downstream signaling marker for TLR3 activation.[31] The level of interferon gamma protein in the supernatant from RPE cells transfected with 10 nM each NI0000, NI0079, NK0000 or NK0144 and that from RPE cells without transfection was below the level of detection (data not shown).

We next compared the effect of canonical double-stranded siRNAs and a new class of RNAi agents on CNV formation *in vivo*. The average CNV volumes at day 7 after the injection of 1 µl of 10 µM of each canonical double-stranded siRNAs (NI0000 or NI0079) tended to be lower than that in the PBS injection group, although the difference between PBS injection group and NI0000 or NI0079 injection group was not significant ($n = 8$; Figure 8c). In contrast, the volume of the CNV in eyes treated with 1 µl of 10 µM NK0000 was not reduced compared with the PBS-treated eyes. An intravitreal injection of 1 µl of 10 µM NK0144 led to significantly smaller volumes of CNV than eyes after 1 µl of 10 µM NK0000 injections (Figures 7a and 8c).

These results indicated that the new class of RNAi agents had no off-target effects and the observed inhibitory effect of CNV by NK0144 was the result of a specific knock-down of POSTN.

No obvious adverse effects by NK0144 on retina

To evaluate retinal function after intravitreal injections of NK0144, we recorded electroretinographies (ERGs) from mice at 21 days after 1 µl of 10 µM NK0144 injection on days 0 and 7. The mean amplitude of the a- and b-waves in the mice eyes treated with

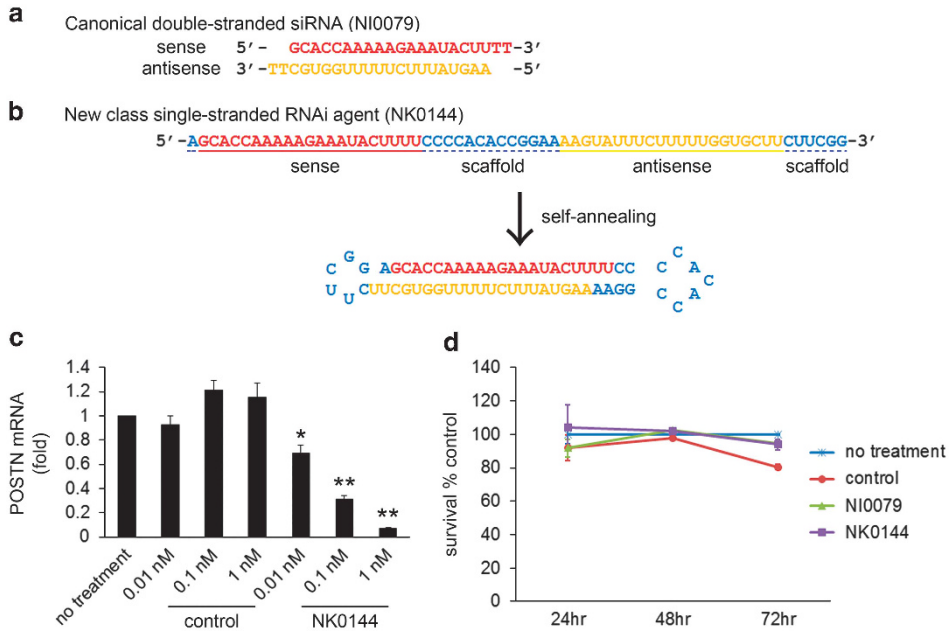

Figure 4. Structure of canonical double-stranded siRNA (**a**) and new class single-stranded RNAi agent (**b**), and the NK0144-mediated effects on *POSTN* mRNA and cell survival in cultured human RPE cells. Cultured RPE cells were transfected or not transfected with negative control siRNA, or NI0079, or NK0144. Total RNA was extracted at 24 h after transfection and was analyzed by real-time RT-PCR (**c**). Cell viability at 24, 48 and 72 h after transfection was assessed by MTT assay (**d**). (**a**) Canonical double-stranded siRNA was prepared as double-stranded RNA oligomers. (**b**) New class of RNAi agent was prepared as single-stranded RNA oligomers that then self-anneal as shown. Nucleotides in red indicate sense strand of the target (POSTN), nucleotides in yellow are the antisense strand, and nucleotides in blue are the scaffold. (**c**) Expression of the mRNA of *POSTN* in ARPE19 cells exposed to 0.01, 0.1 and 1 nM of NK0144 was significantly reduced in a dose-dependent manner compared with those with negative control siRNA treatment ($n = 4$ per group). $^{*}P < 0.05$, $^{**}P < 0.0001$. (**d**) No significant difference in cell viability was observed up to 72 h between RPE cells with NK0144 treatment and those with control siRNA treatment ($n = 4$ per group).

NK0144 (scotopic a-wave = 386.1 ± 13.5 μV, scotopic b-wave = 744.8 ± 59.1 μV) were not significantly different from that of the untreated control eyes (scotopic a-wave = 370.3 ± 10.5 μV, scotopic b-wave = 703.1 ± 55.0 μV; $n = 4$; Figure 9a).

The histological structure observed by hematoxylin and eosin staining of the mouse retina at 21 days after NK0144 injection appeared normal and did not differ from that of the untreated eyes (Figure 9b). The retina of the CNV mouse model showed terminal deoxynucleotidyl transferase dUTP nick end labeling (TUNEL)-positive apoptotic cells in the outer nuclear layer. In contrast, the eyes injected with NK0144 showed no TUNEL-positive staining in the retina (Figure 9c). These results showed that NK0144 had no adverse effects on the function and morphology of the retina.

DISCUSSION

Anti-VEGF therapy has been used to treat the CNV in eyes with AMD, and this treatment has led to significant advances in the understanding of the pathogenesis of AMD.[36–38] However, the CNV activity does not respond to multiple treatments as is required in many patients. In addition, there is currently no therapy to treat choroidal fibrosis. Therefore, finding additional therapeutic methods is still a goal.

To the best of our knowledge, this is the first study providing evidence that POSTN is expressed in choroidal FVMs in both a CNV mouse model and AMD patients. Furthermore, our results showed the usefulness of a new class of single-stranded RNAi molecule that targeted POSTN and can be considered for the treatment of choroidal FVMs. Intravitreal injections of NK0144 significantly inhibited the volume of the induced CNVs and subsequent fibrosis, which supports our findings that POSTN is a positive regulator of choroidal FVMs formation.

Our data demonstrated that POSTN is expressed by the RPE cells associated with choroidal FVMs in both a CNV mouse model and AMD patients. Moreover, genetic ablation of *Postn* gene can inhibit both CNV and choroidal fibrosis. Thus, an elevated expression of POSTN by RPE cells may promote the development of choroidal FVMs. These findings are in line with our earlier reports showing that the POSTN produced by RPE cells in eyes with proliferative vitreoretinopathy promotes preretinal fibrous proliferation of RPE cells through integrin α_v-mediated focal adhesion kinase in an autocrine manner.[17,18,20] In addition, because integrin $\alpha_v\beta_3$ is involved in the development of CNVs in eyes with AMD,[39,40] the POSTN expressed by RPE cells may also promote CNV development through integrin $\alpha_v\beta_3$ in a paracrine manner.

It was recently reported that anti-VEGF therapy may have a role in the development of geographic atrophy in AMD patients compared with that following other treatments.[16] This is partly because VEGF has an important role in the normal function of the retina and the maintenance of the choriocapillaris.[41] Thus, the therapies that block VEGF to inhibit pathologic neovascularization could result in unexpected disturbances of the normal homeostasis in the retina and should be used cautiously. In contrast to VEGF, we have reported that the mRNA and protein of POSTN were barely detectable in the normal retina.[20] Together with the fact that anti-POSTN therapy in this study showed no apparent adverse effects, these results raise the possibility that POSTN may be an attractive therapeutic target to regulate 'disease-specific' pathways involved in the development of choroidal FVMs, while minimizing the unfavorable side effects to the normal retina.

Although canonical double-stranded siRNAs have attractive and promising aspects for new therapy, some obstacles still remain to be overcome before their clinical application.[30] These hurdles include the lack of a safe DDS, adverse off-target effects through TLR3 activation and the lack of stability. In this study, we tried to

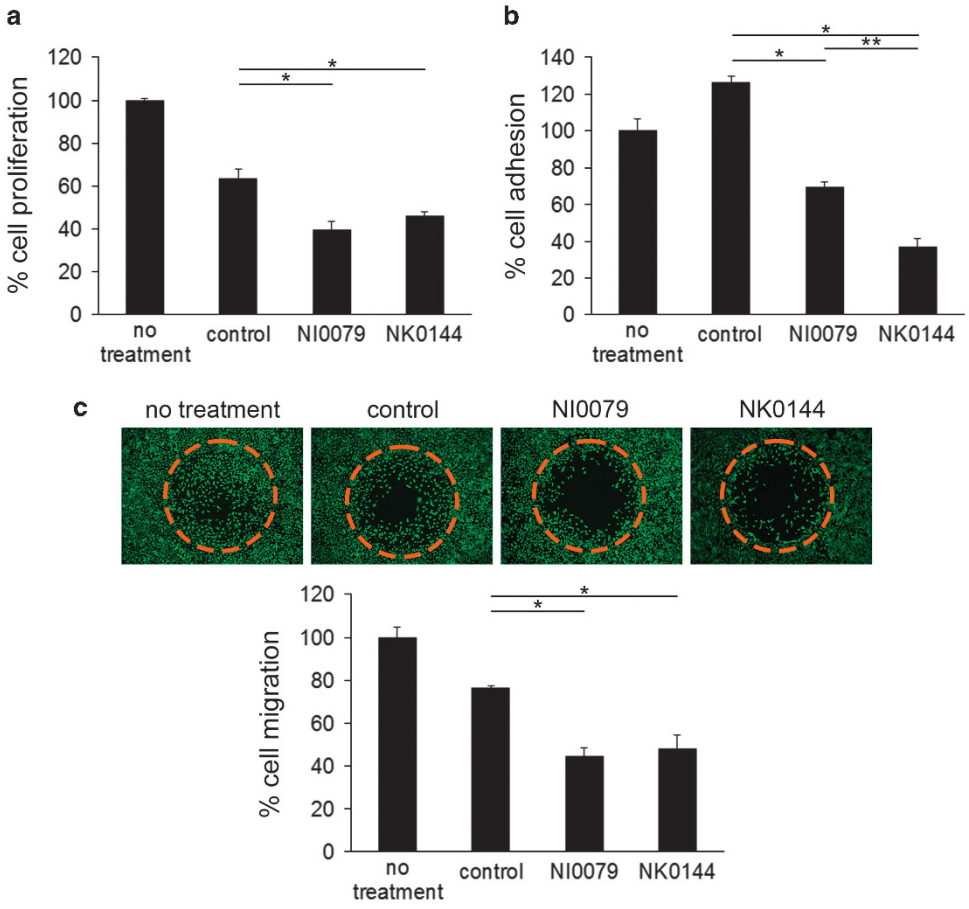

Figure 5. NK0144-mediated effects on human RPE cell proliferation, adhesion and migration *in vitro*. BrdU-ELISA was used to assess the transfected cell proliferation, and MTT assay was used to assess cell migration. The migration of RPE cells was examined on fibronectin-coated well after 48-h incubation by staining with calcein AM and quantified with a fluorescence microplate reader. (**a**) NK0144 significantly inhibited the proliferation of human RPE compared with negative control siRNA ($n = 4$ per group). $^{*}P < 0.01$. (**b**) Human RPE cells adhesion was reduced more by NK0144 transfection than by both negative control siRNA and NI0079 ($n = 4$ per group). $^{*}P < 0.001$, $^{**}P < 0.01$. (**c**) NK0144 significantly reduced the degree of migration of human RPE cells more than that with negative control siRNA ($n = 4$ per group). $^{*}P < 0.01$.

overcome these obstacles by using a new class of single-stranded RNAi agents that self-anneals into a unique structure containing a canonical double-stranded RNA. Previous studies showed that the new single-stranded RNAi is not associated with off-target effect and is more stable against nuclease than canonical double-stranded siRNA.[35,42] Our results showed that naked NK0144 can significantly inhibit the expression of POSTN, proliferation, adhesion and migration of RPE cells without target sequence-independent effect through TLR3 activation and influence on cell viability. Furthermore, we showed that labeled single-stranded nkRNA without any DDS was detected in the RPE-choroid for at least 5 days following an intravitreal injection. This suggests that it was taken up and retained within cells at the CNV site for a substantial period of time. Unlike canonical double-stranded siRNAs, we also demonstrated that naked NK0144 significantly inhibited choroidal FVM formation and had POSTN sequence-dependent CNV suppression without serious toxicity. These results strongly indicate that intravitreal injections of naked NK0144 may be a safer and more efficient therapeutic method to inhibit choroidal CNV. This is because the naked single-stranded RNAi therapy may be safer than canonical siRNA because of its stability, no DDS need, and much less proinflammatory or toxicological responses induced by siRNA itself or by accompanying DDS.[43] Unlike previous reports, target sequence-independent CNV suppression by canonical siRNAs was not significant in this study. This is probably due to the smaller injection amounts of canonical double-stranded siRNAs (0.1 μg per eye). In the previous reports, the inhibitory effect was only observed with the 10 times larger amount (1 μg per eye).[31]

In conclusion, our results show a causal link between POSTN and choroidal FVM formation, and the effects of a naked, unmodified new class of RNAi agent targeting POSTN. Additional preclinical studies concerning the toxicity, stability and effect of duration are underway for establishing the new POSTN-targeting RNAi agent for combating choroidal FVM formation.

MATERIALS AND METHODS

Animals

All animal experiments were performed following the guidelines of the Association for Research in Vision and Ophthalmology (ARVO) Statement on the Use of Animals in Ophthalmic and Vision Research. The experimental protocols were approved by the Institutional Animal Care and Use Committee of Kyushu University.

C57BL/6J WT mice (CLEA, Tokyo, Japan) and *Postn* KO mice between 6 and 8 weeks were used for the animal experiments. PCR was used to determine the genotype of the experimental mice. Primer sequences for genotyping were as follows:

5′-GTTCTTACAGAAAGCAGAAGGATAC-3′ and
5′-TTAAATCACTCCACAGCAGAACACG-3′
were used to detect a 436-bp product for the WT allele; and
5′-CATGATAGCTTCTCTCCCAGTTCTC-3′ and
5′-CTTGCAATAAGTAAAACAGCTCCCC-3′
were used to detect a 372-bp product for the *Postn* KO allele.

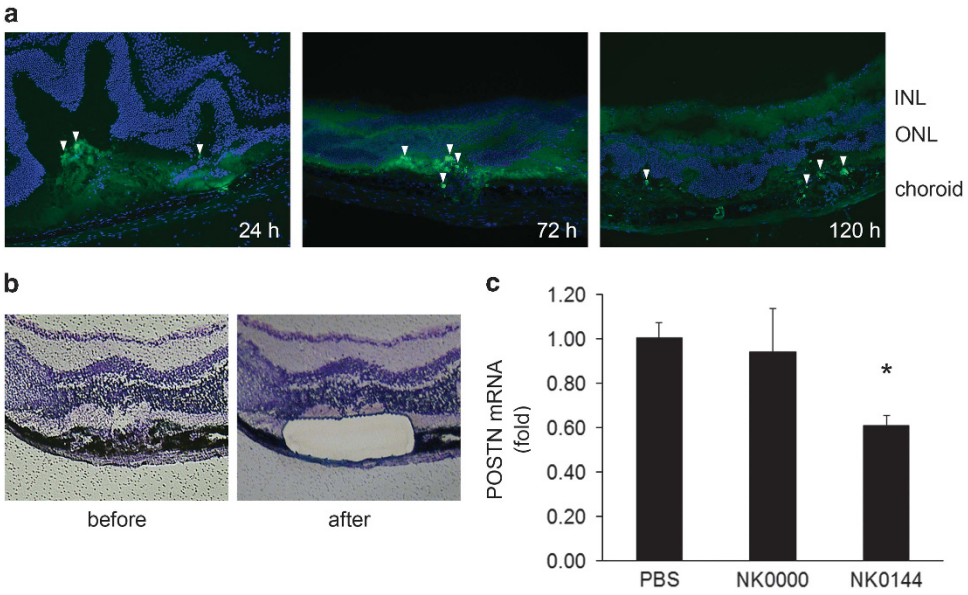

Figure 6. Distribution of FITC-labeled NK0144 in the mouse retina at different time points after intravitreal injection (**a**) and inhibitory effect of NK0144 on the expression of *Postn* mRNA *in vivo* (**b**, **c**). FITC-labeled NK0144 was given by intravitreal injection at the same time as laser treatment. The mice were killed at 24, 72, 120 h after the injection. The eyes were enucleated and cryosections were cut, and the cell nuclei were stained with DAPI (blue) followed by examination by fluorescence microscopy. The mRNAs at CNV sites were extracted using laser-capture microdissection at day 14 and analyzed by real-time RT-PCR. (**a**) NK0144 (green) can be clearly seen at the CNV site from 24 h after intravitreal injection. The staining for NK0144 at the laser site increased at 72 h, and decreased at 120 h although it was still detectable. (**b**) Immunostaining before (left) and after (right) laser microdissection. (**c**) The level of *Postn* mRNA in CNV site was significantly decreased by intravitreal injection of 10 μM NK0144 compared with NK0000 injection group and PBS injection group ($n = 4$ per group). $^*P < 0.05$.

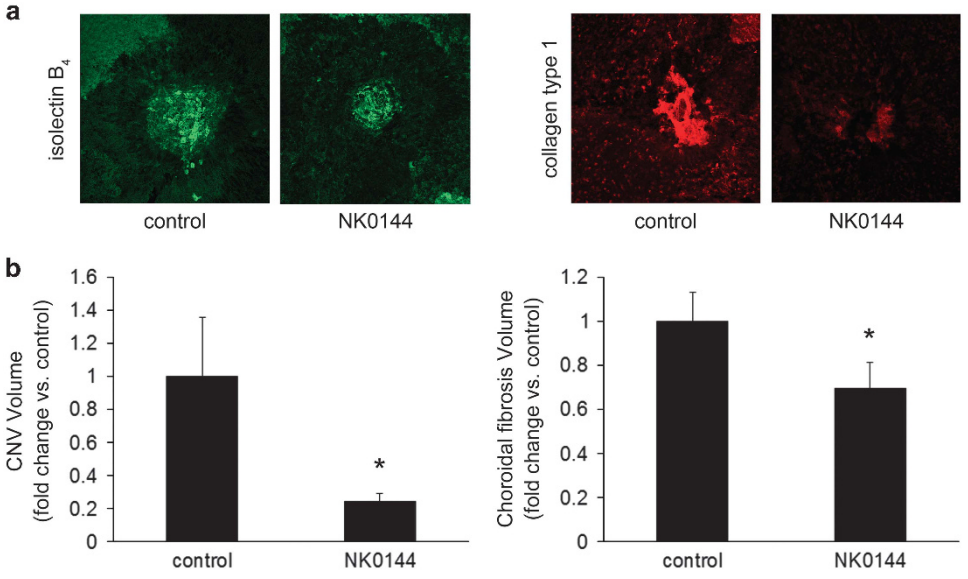

Figure 7. Effect of NK0144 on progression of CNV at day 7 and choroidal fibrosis at day 21 in laser-induced CNV mouse model. On days 0 or 7 after CNV induction, mice were injected intravitreally with 1 μl of 10 μM negative control siRNA in one eye and 1 μl of 10 μM of NK0144 in the fellow eye. The mice were killed 7 days after the injection for CNV and 21 days after injection for choroidal fibrosis assessments. The eyes were enucleated and choroidal flat mounts were stained with isolectin B4 and collagen type I and examined by laser scanning confocal microscopy. (**a**) Representative immunohistochemical analysis shows that the areas of CNV and choroidal fibrosis in NK0144 treatment group were smaller than those in negative control siRNA treatment group. (**b**) Both CNV and choroidal fibrosis volumes in eyes treated with NK0144 were significantly smaller than that in the negative control siRNA group (NK0000; $n = 8$ per group). $^*P < 0.05$.

Laser-induced CNV model

CNVs were generated as described in detail.[44] Briefly, mice were anesthetized with intraperitoneal injections of 100 mg kg^{-1} ketamine and 10 mg kg^{-1} xylazine, and the pupils were dilated with a mixture of 0.5% tropicamide and 0.5% phenylephrine hydrochloride (Mydrin P; Santen, Osaka, Japan). Laser photocoagulation (532 nm, 100 mW, 100 ms, 75 μm; Verdi; Coherent, Santa Clara, CA, USA) was applied to each fundus using a coverslip as a contact lens on day 0 (4–6 shots per eye for CNV volume studies: 20 shots per eye for mRNA and protein analyses). The formation of a bubble at the time of laser application indicating a rupture of Bruch's membrane was an important sign that sufficient injury had been done to induce a CNV. Thus, only burns with bubble were included in the study. We excluded burns with bleeding.

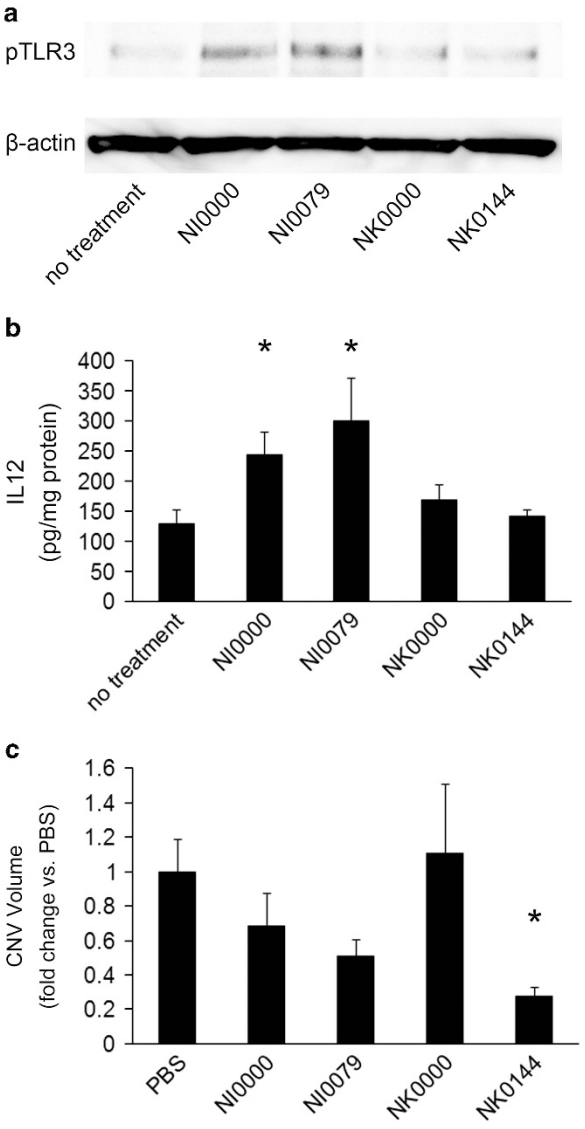

Figure 8. RNAi agent-mediated effects on TLR3 phosphorylation and IL-12 levels in cultured human RPE cells *in vitro,* and target sequence-independent CNV suppression *in vivo*. *In vitro*, cultured RPE cells were transfected or not transfected with NI0000, NI0079, NK0000 or NK0144. Total protein was extracted at 30 min after transfection for western blot (**a**) or 24 h after transfection for ELISA (**b**). *In vivo*, mice were injected intravitreally with 1 μl of 10 μM each RNAi agents on day 0 after CNV induction. CNV volumes 7 days after the injection were analyzed using choroidal flat mounts stained with isolectin B4 (**c**). (**a**) TLR3 phosphorylation was detected in RPE cells after exposure to NI0000 or NI0079, whereas NK0000 and NK0144 had no effect on TLR3 phosphorylation. β-Actin served as loading control. (**b**) IL-12 levels in RPE cells exposed to NI0000 or NI0079 were significant higher, whereas no significant difference was observed between RPE cells without treatment and those transfected with NK0000 or NK0144 ($n = 4$ per group). *$P < 0.05$. (**c**) Target sequence-independent CNV suppression was observed in the double-stranded scrambled siRNA (NI0000) injection group, whereas there was no decrease of CNV in the corresponding single-stranded scrambled RNAi (NK0000) injection groups compared with PBS injection group ($n = 8$ per group). Intravitreal injection of NK0144 showed significantly smaller areas of CNV than eyes after NK0000 injections. *$P < 0.05$.

Human specimens

Choroidal FVM was isolated from the sensory retina and RPE using 33G subretinal canula and incised from the subretinal space of patients with AMD who were undergoing pars plana vitrectomy.

Quantitative real-time RT-PCR

Total RNA was extracted from the homogenized RPE-choroid complexes at the selected time points and the human RPE cells treated with RNAi agents. The MagDEA RNA kit (Precision System Science, Pleasanton, CA, USA) was used according to the manufacturer's protocol.[44,45] After quantification of the RNA concentration, complementary DNAs were synthesized with a First Strand cDNA Synthesis Kit (Roche, Mannheim, Germany). Quantitative RT-PCR was performed and analyzed using a SYBR Premix Ex Taq (Takara, Shiga, Japan) and a LightCycler 96 PCR system (Roche). A volume of 20 μl containing 0.2 μM of primers was loaded into each LightCycler well. The primer sequences were as follows:

for mouse *Postn,*
5′-CTTTCGAGAAACTGCCACGAG-3′ and
5′-CCTTCCATGGTCTCAAACACG-3′;
for mouse β-actin,
5′-GATGACCCAGATCATGTTTGA-3′ and
5′-GGAGAGCATAGCCCTCGTAG-3′;
for human *POSTN*,
5′-TGCCCAGCAGTTTTGCCCAT-3′ and
5′-CGTTGCTCTCCAAACCTCTA-3′;
and for human β-actin,
5′-ATAGCACAGCCTGGATAGCAACGTAC-3′ and 5′-CACCTTCTACAATGAGCTGCGTGTG-3′.

The quality and specificity of the PCR reaction were determined by melting curves. A standard curve was used to quantify the expression levels.

Enzyme-linked immunosorbent assay

Total protein was isolated from the sonicated RPE-choroid complexes using Tissue Protein Extraction Reagent with protease inhibitor (T-PER; Thermo, Waltham, MA, USA). The concentrations of POSTN in the mouse RPE-choroid complexes, and IL-12 and interferon gamma in the supernatant from the cultured human RPE cells were measured with a mouse POSTN immunoassay kit (R&D Systems, Minneapolis, MN, USA), human IL-12 ELISA kit (Thermo) and human interferon gamma immunoassay kit (R&D Systems), respectively, according to the manufacturer's instructions.

Immunohistochemistry

Eyes enucleated from a CNV mouse model and human choroidal FVMs resected during vitrectomy were fixed in 4% paraformaldehyde, then embedded in paraffin and cut at 3 μm thickness. After deparaffinization, rehydration and blocking, the sections were incubated with the primary antibodies overnight at 4 °C, and the second antibodies were added for 1 h at room temperature. Nuclei were counterstained with 4,6-diamidino-2-phenylindole (DAPI; Hoechst 33342; Molecular Probes, Eugene, OR, USA). After washing with PBS, the cover slides were mounted with an aqueous mounting medium (Thermo). A fluorescent microscope (BZ-9000; KEYENCE, Osaka, Japan) was used to examine and analyze the specimens.[46–48]

The primary antibodies were POSTN (MAB 3548: 5 μg ml^{-1}; R&D Systems), RPE65 (MAB 5428: 5 μg ml^{-1}; Millipore, Temecula, CA, USA) and pan-cytokeratin (sc-8018: 1:100 dilution; Santa Cruz, Dallas, TX, USA). The second antibodies were Alexa Fluor 488 and 647 (1:100 dilution; Molecular Probes).

CNV and choroidal fibrosis volume measurement

The volumes of the CNVs on day 7 and that of the choroidal fibrous tissue on day 21 after laser photocoagulations were measured in choroidal flat mounts. Choroidal flat mounts were prepared as described in detail.[44] Briefly after fixation in 4% paraformaldehyde, the cornea, lens and neurosensory retina of the enucleated eyes were removed from the eye. The remaining eyecups were washed with PBS and placed in 50 and 100% methanol for 10 min each at room temperature. The samples were then placed in PBS containing 1% bovine serum albumin and 0.5% TritonX-100 as a blocking buffer for 1 h at room temperature. This was followed by incubation with the primary antibodies overnight at 4 °C and second antibodies for 1 h at room temperature. Several radial cuts were made from the edge to the equator and the eyecups were flat mounted in mounting medium. Choroidal flat mounts were observed with a laser scanning confocal microscope (Nikon A1; Nikon, Tokyo, Japan), and the volumes at each burn were measured using a software (NIS-Elements Software; Nikon).

The primary antibodies were fluorescein-labeled isolectin B4 (FL1201; 1:200 dilution; Vector Laboratories, Burlingame, CA, USA) for CNV and

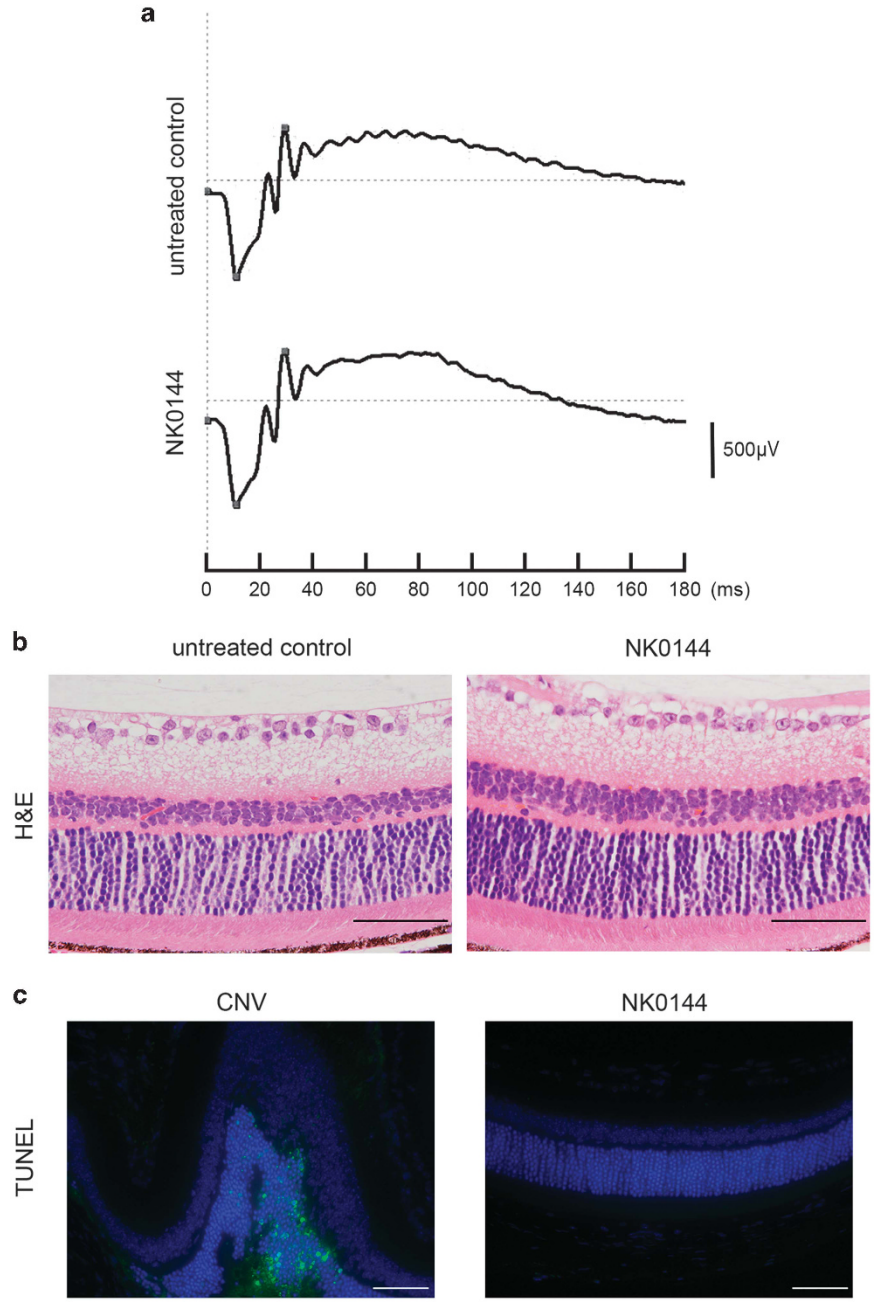

Figure 9. Absence of apparent adverse effects of NK0144 intravitreal injection on function and morphology in mouse retinas. Intravitreal injection of NK0144 was performed on days 0 and 7. (**a**) Scotopic ERGs recorded on day 21 in eyes without any treatment and eyes with NK0144 treatment. The differences in the amplitudes of the a-wave and b-wave between untreated group and NK0144 treatment group were not significant ($n = 4$). (**b**) Hematoxylin and eosin (H&E) staining of retinas obtained on day 21 from mice with NK0144 treatment appeared normal as well as those from untreated mice. (**c**) TUNEL staining of retinas from CNV model mice (left) was used as a TUNEL-positive control. No TUNEL-positive cells were observed in retinas of eyes at 21 days after NK0144 treatment (right). Scale bars = 50 μm.

collagen type I (600-401-103; 1:100 dilution; ROCKLAND, Gilbertsville, PA, USA) for choroidal fibrous tissue. The second antibody for collagen type I was Alexa Fluor 647 (1:100 dilution; Molecular Probes).

Preparation of new class of RNAi agent targeting POSTN

New RNAi agents were synthesized on solid phase as single-stranded RNAs as described in detail.[35] NI0079 was a canonical double-stranded siRNA designed to target the mRNA of human and mouse *Postn* (Figure 4a), and NI0000 was a scrambled double-stranded siRNA. A long single-stranded oligonucleotides, denoted as NK0144, was constructed by incorporating the sense and antisense nucleotides of NI0079 into the scaffold of a unique RNAi platform named nkRNA (Figure 4b).[35] The nkRNAs are new class of RNAi agents that spontaneously anneal to form a helical structure containing a double-stranded central stem and two loops within a molecule.[35] NK0000 was also a new class of RNAi agent, but the sequences were scrambled. The sequences of the RNAi agents were described in detail in Table 1.

Cell culture and transfection

Cells from the ARPE19 cell line and human primary RPE cells isolated from fetal human eyes (Lonza, Walkersville, MD, USA) were used for the *in vitro* studies. Cells were cultured in Dulbecco's modified Eagle's medium (DMEM) containing 100 U ml^{-1} penicillin, 100 μg ml^{-1} streptomycin and 10% heat-inactivated fetal bovine serum at 37 °C in 5% CO_2.

When the cultured cells in 24-well plates were 50–70% confluent, they were transfected with canonical double-stranded siRNA (NI0079), or the new single-stranded RNAi agent (NK0144) for POSTN, or a negative control RNAi. The incubation time for the transfection was 24 h using the RNAi MAX reagent (Invitrogen, Carlsbad, CA, USA) according to the manufacturer's protocol. The final concentrations of RNAi agents were 0.01, 0.1 and 1 nM to determine the knock-down effect of NK0144 transfection on the expression of *POSTN* in ARPE19 cells. To assay the primary RPE cells, a final concentration of 10 nM RNAi agents was chosen. The reagent mixtures for transfection were replaced by DMEM containing 3% fetal bovine serum with recombinant TGF-β2 at a final concentration of 3 ng ml^{-1} as the inducer of POSTN, followed by each assay.

Cell viability and adhesion assay (MTT assay)

Cell viability was assessed at 24, 48 and 72 h after transfection by staining with 3-(4,5-dimethyl-2-thiazolyl)-2,5-diphenyl-2H tetrazolium bromide (MTT: 5 mg ml^{-1}; Sigma-Aldrich, St Louis, MO, USA) as described in detail.[49] In brief, the reagent mixture for transfection was removed and fresh medium with 5 mg ml^{-1} MTT was added for 5 h to detect live cells.

The MTT assay was also used to measure cell adhesion as described.[20] Briefly, transfected RPE cells were placed in DMEM containing 3% fetal bovine serum and recombinant TGF-β2 for 24 h. The cells were then trypsinized and 1×10^4 cells were injected on fibronectin-coated wells and allowed to attach for 60 min. After washing gently with PBS twice, fresh medium with 5 mg ml^{-1} MTT was added for 5 h.

Each MTT assay was quantified by measuring the level of formazan precipitates using 100% DMSO (Sigma-Aldrich). The absorbance at 590 nm was measured using an Immuno Mini NJ-2300 plate reader (NJ InterMed, Tokyo, Japan).

Cell proliferation assay

For cell proliferation assays, 1×10^4 transfected RPE cells were seeded in each well of 96-well plates and incubated with TGF-β2. After 24 h, bromodeoxyuridine (BrdU)-ELISA (Roche) was used to assess the cell proliferation according to the manufacturer's instructions.

Cell migration assay

The Oris 96-well cell migration assay kit (Platypus Technologies, Madison, WI, USA) was used to assess the degree of cell migration according to the manufacturer's instructions. Briefly, 5×10^4 RPE cells were seeded in each fibronectin-coated well and transfected with each RNAi agents. After 1 h of pretreatment in DMEM with 3% fetal bovine serum containing recombinant TGF-β2 and 5 μg ml^{-1} aphidicolin (Sigma-Aldrich) to inhibit cell division, the stoppers were removed to start the migration of cells into the detection zone. After 48 h from the initiating of migration, the cells were stained with DMEM containing calcein AM (2 μg ml^{-1}, Molecular Probes) for 1 h. Then, the signal intensity of the stained cells that migrated into the detection zone was measured with a Spectra Max M5 microplate reader in the fluorescence mode (Molecular Devices, Sunnydale, CA, USA). The fluorescence filter set (excitation 485 nm and emission 528 nm) with an Oris detection mask attached to the bottom of the plate was used.

POSTN RNAi treatment *in vivo*

Immediately after the laser photocoagulation, mice were given an intravitreal injection of 1 μl PBS containing 10 μM of control siRNA in one eye and NK0144 in the fellow eye. An additional injection was given on day 7 for the choroidal fibrosis volume assessments. The intravitreal injections were performed 0.5 mm away from the limbus using a 1 ml Hamilton syringe (Hamilton, Reno, NV, USA) and a 33-gauge needle under a surgical microscope.

Assessment of distribution of FITC-labeled NK0144 in retina after intravitreal injections

Mice that received an intravitreal injection of FITC-labeled NK0144 were killed at 24, 72 and 120 h after the injection, and the enucleated eyes were frozen in optimal cutting temperature embedding compound (OCT compound; Sakura Finetek, Tokyo, Japan). Then, 10 μm thick frozen sections were cut with a cryostat and fixed in acetone. After blocking with 3% skim milk, the nuclei were stained with DAPI and mounted with aqueous mounting medium. The sections were examined with a fluorescent microscope.

Laser-capture microdissection

Laser-capture microdissection was used to purify the CNV sites from whole retinas. Eyes from mice injected with each RNAi agents were enucleated at day 14 and embedded in OCT compound (4583; Sakura Finetech) and kept at −80 °C until sectioning. Then, 10 μm thick sections were cut with a cryostat and placed on glass slides designed for laser microdissection microscopy (LMD6500; Leica Microsystems, Wetzlar, Germany). Sections were stained with toluidine blue and only CNV sites were collected by laser microdissection.

Western blot analysis

RPE cells were seeded in collagen-coated six-well plates. After starvation with serum-free DMEM for 24 h, the cells were transfected with each RNAi agents. After 30-min incubation, the total cell lysates were extracted using lysis buffer with protease inhibitor and phosphatase inhibitor (Thermo). The extracted cell lysates were subjected to 4–12% sodium dodecyl sulfate-NuPAGE, and the blots were incubated with an Ab against phosphorylated TLR3 (Tyr759, NBP2-24904: 0.1 μg ml^{-1}; Novus Biologicals, Littleton, CO, USA). Visualization was performed using a SuperSignal West Femto Maximum Sensitivity Substrate (Thermo) detection system. Lane-loading differences were determined by blotting the membranes with an Ab against β-actin (4970: 1:1000; Cell Signaling Technology, Danvers, MA, USA).

Electroretinography

ERGs were recorded as described in detail.[50] Briefly, mice were dark-adapted overnight and were anesthesized under dim red light. The pupils were dilated and recordings were made using the PuREC system (MAYO, Aichi, Japan). ERGs were recorded on day 21 after the intravitreal injections of 1 μl PBS containing 100 pmol NK0144 on days 0 and 7. The ERGs of the untreated eyes were used as controls. The scotopic ERGs were elicited by a stimulus intensity of 10 000 cd m^{-2}, and the responses were differentially amplified and filtered between 0.3 and 500 Hz.

Histology and TUNEL

Hematoxylin and eosin and TUNEL staining of paraffin-embedded sections were performed. An ApopTag Fluorescein *In Situ* Apoptosis Detection Kit (Millipore) was used for the TUNEL staining, and the procedures were according to the manufacturer's protocol. The sections were costained with DAPI (Molecular Probes) to observe the cell nuclei, and the stained sections were examined under a fluorescence microscope. A retina from the mouse CNV model was used as a TUNEL-positive control.

Statistical analyses

All results are expressed as the means ± s.e.m. All statistical analyses of the differences between groups were made using the Dunnett's test or Wilcoxon rank sum test. Differences were considered significant for $P < 0.05$. Statistical analyses were performed using JMP 9.0.2 (SAS Institute, Cary, NC, USA).

CONFLICT OF INTEREST

The patent on periostin (WPO Patent WO/2013/147140) became public, and in these patents, the names of TN, SY, KI, TH, TO and TI are included. This work was supported in part by A-STEP (Adaptable & Seamless Technology Transfer Program through Target-driven R&D) governed by Japan Science and Technology Agency. SY is supported by JSPS 26293374. KT, AS and KY are employees of AQUA Therapeutics and hold equity. TH, TO and HH are employees of BONAC Corporation and hold equity. The remaining authors declare no conflict of interest.

ACKNOWLEDGEMENTS

We thank the staff of the Research Support Center (Graduate School of Medical Sciences, Kyushu University) for technical support and Masayo Eto, Kinuko Sasada and Hiroko Miura for their excellent technical assistance. This work was supported in part by JSPS KAKENHI grant numbers 24249083, 23592574, 26293374, 26670757, Takeda Science Foundation, and Adaptable and Seamless Technology Transfer Program through Target-driven R&D from the Japan Science and Technology Agency. T Nakama is supported by a fellowship from the Japan Society for the Promotion of Science for Young Scientists.

REFERENCES

1 Friedman DS, O'Colmain BJ, Munoz B, Tomany SC, McCarty C, de Jong PT *et al.* Prevalence of age-related macular degeneration in the United States. *Arch Ophthalmol* 2004; **122**: 564–572.
2 de Jong PT. Age-related macular degeneration. *N Engl J Med* 2006; **355**: 1474–1485.
3 Nakata I, Yamashiro K, Nakanishi H, Akagi-Kurashige Y, Miyake M, Tsujikawa A *et al.* Prevalence and characteristics of age-related macular degeneration in the Japanese population: the Nagahama study. *Am J Ophthalmol* 2013; **156**: 1002–1009 e2.
4 Chandra SR, Gragoudas ES, Friedman E, Van Buskirk EM, Klein ML. Natural history of disciform degeneration of the macula. *Am J Ophthalmol* 1974; **78**: 579–582.
5 Hogg R, Curry E, Muldrew A, Winder J, Stevenson M, McClure M *et al.* Identification of lesion components that influence visual function in age related macular degeneration. *Br J Ophthalmol* 2003; **87**: 609–614.
6 Schlingemann RO. Role of growth factors and the wound healing response in age-related macular degeneration. *Graefes Arch Clin Exp Ophthalmol* 2004; **242**: 91–101.
7 Penfold PL, Killingsworth MC, Sarks SH. Senile macular degeneration: the involvement of immunocompetent cells. *Graefes Arch Clin Exp Ophthalmol* 1985; **223**: 69–76.
8 Bloch SB, Lund-Andersen H, Sander B, Larsen M. Subfoveal fibrosis in eyes with neovascular age-related macular degeneration treated with intravitreal ranibizumab. *Am J Ophthalmol* 2013; **156**: 116–124 e1.
9 Lopez PF, Grossniklaus HE, Lambert HM, Aaberg TM, Capone Jr A, Sternberg Jr P *et al.* Pathologic features of surgically excised subretinal neovascular membranes in age-related macular degeneration. *Am J Ophthalmol* 1991; **112**: 647–656.
10 Grossniklaus HE, Martinez JA, Brown VB, Lambert HM, Sternberg Jr P, Capone Jr A *et al.* Immunohistochemical and histochemical properties of surgically excised subretinal neovascular membranes in age-related macular degeneration. *Am J Ophthalmol* 1992; **114**: 464–472.
11 Watanabe D, Takagi H, Suzuma K, Oh H, Ohashi H, Honda Y. Expression of connective tissue growth factor and its potential role in choroidal neovascularization. *Retina* 2005; **25**: 911–918.
12 Nagineni CN, Samuel W, Nagineni S, Pardhasaradhi K, Wiggert B, Detrick B *et al.* Transforming growth factor-beta induces expression of vascular endothelial growth factor in human retinal pigment epithelial cells: involvement of mitogen-activated protein kinases. *J Cell Physiol* 2003; **197**: 453–462.
13 Recalde S, Zarranz-Ventura J, Fernandez-Robredo P, Garcia-Gomez PJ, Salinas-Alaman A, Borras-Cuesta F *et al.* Transforming growth factor-beta inhibition decreases diode laser-induced choroidal neovascularization development in rats: P17 and P144 peptides. *Invest Ophthalmol Vis Sci* 2011; **52**: 7090–7097.
14 Daniel E, Toth CA, Grunwald JE, Jaffe GJ, Martin DF, Fine SL *et al.* Risk of scar in the comparison of age-related macular degeneration treatments trials. *Ophthalmology* 2014; **121**: 656–666.
15 Hwang JC, Del Priore LV, Freund KB, Chang S, Iranmanesh R. Development of subretinal fibrosis after anti-VEGF treatment in neovascular age-related macular degeneration. *Ophthalmic Surg Lasers Imaging* 2011; **42**: 6–11.
16 Grunwald JE, Daniel E, Huang J, Ying GS, Maguire MG, Toth CA *et al.* Risk of geographic atrophy in the comparison of age-related macular degeneration treatments trials. *Ophthalmology* 2014; **121**: 150–161.
17 Yoshida S, Ogura A, Ishikawa K, Yoshida A, Kohno R, Yamaji Y *et al.* Gene expression profile of fibrovascular membranes from patients with proliferative diabetic retinopathy. *Br J Ophthalmol* 2010; **94**: 795–801.
18 Yoshida S, Ishikawa K, Asato R, Arima M, Sassa Y, Yoshida A *et al.* Increased expression of periostin in vitreous and fibrovascular membranes obtained from patients with proliferative diabetic retinopathy. *Invest Ophthalmol Vis Sci* 2011; **52**: 5670–5678.
19 Asato R, Yoshida S, Ogura A, Nakama T, Ishikawa K, Nakao S *et al.* Comparison of gene expression profile of epiretinal membranes obtained from eyes with proliferative vitreoretinopathy to that of secondary epiretinal membranes. *PLoS One* 2013; **8**: e54191.
20 Ishikawa K, Yoshida S, Nakao S, Nakama T, Kita T, Asato R *et al.* Periostin promotes the generation of fibrous membranes in proliferative vitreoretinopathy. *FASEB J* 2014; **28**: 131–142.
21 Kudo A. Periostin in fibrillogenesis for tissue regeneration: periostin actions inside and outside the cell. *Cell Mol Life Sci* 2011; **68**: 3201–3207.
22 Conway SJ, Izuhara K, Kudo Y, Litvin J, Markwald R, Ouyang G *et al.* The role of periostin in tissue remodeling across health and disease. *Cell Mol Life Sci* 2014; **71**: 1279–1288.
23 Rios H, Koushik SV, Wang H, Wang J, Zhou HM, Lindsley A *et al.* periostin null mice exhibit dwarfism, incisor enamel defects, and an early-onset periodontal disease-like phenotype. *Mol Cell Biol* 2005; **25**: 11131–11144.
24 Snider P, Hinton RB, Moreno-Rodriguez RA, Wang J, Rogers R, Lindsley A *et al.* Periostin is required for maturation and extracellular matrix stabilization of noncardiomyocyte lineages of the heart. *Circ Res* 2008; **102**: 752–760.
25 Malanchi I, Santamaria-Martinez A, Susanto E, Peng H, Lehr HA, Delaloye JF *et al.* Interactions between cancer stem cells and their niche govern metastatic colonization. *Nature* 2012; **481**: 85–89.
26 Shimazaki M, Nakamura K, Kii I, Kashima T, Amizuka N, Li M *et al.* Periostin is essential for cardiac healing after acute myocardial infarction. *J Exp Med* 2008; **205**: 295–303.
27 Ontsuka K, Kotobuki Y, Shiraishi H, Serada S, Ohta S, Tanemura A *et al.* Periostin, a matricellular protein, accelerates cutaneous wound repair by activating dermal fibroblasts. *Exp Dermatol* 2012; **21**: 331–336.
28 Masuoka M, Shiraishi H, Ohta S, Suzuki S, Arima K, Aoki S *et al.* Periostin promotes chronic allergic inflammation in response to Th2 cytokines. *J Clin Invest* 2012; **122**: 2590–2600.
29 Elbashir SM, Harborth J, Lendeckel W, Yalcin A, Weber K, Tuschl T. Duplexes of 21-nucleotide RNAs mediate RNA interference in cultured mammalian cells. *Nature* 2001; **411**: 494–498.
30 Pecot CV, Calin GA, Coleman RL, Lopez-Berestein G, Sood AK. RNA interference in the clinic: challenges and future directions. *Nat Rev Cancer* 2011; **11**: 59–67.
31 Kleinman ME, Yamada K, Takeda A, Chandrasekaran V, Nozaki M, Baffi JZ *et al.* Sequence- and target-independent angiogenesis suppression by siRNA via TLR3. *Nature* 2008; **452**: 591–597.
32 Yang Z, Stratton C, Francis PJ, Kleinman ME, Tan PL, Gibbs D *et al.* Toll-like receptor 3 and geographic atrophy in age-related macular degeneration. *N Engl J Med* 2008; **359**: 1456–1463.
33 Cho WG, Albuquerque RJ, Kleinman ME, Tarallo V, Greco A, Nozaki M *et al.* Small interfering RNA-induced TLR3 activation inhibits blood and lymphatic vessel growth. *Proc Natl Acad Sci USA* 2009; **106**: 7137–7142.
34 Kleinman ME, Kaneko H, Cho WG, Dridi S, Fowler BJ, Blandford AD *et al.* Short-interfering RNAs induce retinal degeneration via TLR3 and IRF3. *Mol Ther* 2012; **20**: 101–108.
35 Hamasaki T, Suzuki H, Shirohzu H, Matsumoto T, D'Alessandro-Gabazza CN, Gil-Bernabe P *et al.* Efficacy of a novel class of RNA interference therapeutic agents. *PLoS One* 2012; **7**: e42655.
36 Rosenfeld PJ, Brown DM, Heier JS, Boyer DS, Kaiser PK, Chung CY *et al.* Ranibizumab for neovascular age-related macular degeneration. *N Engl J Med* 2006; **355**: 1419–1431.
37 Gragoudas ES, Adamis AP, Cunningham Jr ET, Feinsod M, Guyer DRGroup VISiONCT. Pegaptanib for neovascular age-related macular degeneration. *N Engl J Med* 2004; **351**: 2805–2816.
38 Stewart MW, Rosenfeld PJ. Predicted biological activity of intravitreal VEGF Trap. *Br J Ophthalmol* 2008; **92**: 667–668.
39 Mousa SA, Lorelli W, Campochiaro PA. Role of hypoxia and extracellular matrix-integrin binding in the modulation of angiogenic growth factors secretion by retinal pigmented epithelial cells. *J Cell Biochem* 1999; **74**: 135–143.
40 Friedlander M, Theesfeld CL, Sugita M, Fruttiger M, Thomas MA, Chang S *et al.* Involvement of integrins alpha v beta 3 and alpha v beta 5 in ocular neovascular diseases. *Proc Natl Acad Sci USA* 1996; **93**: 9764–9769.
41 Saint-Geniez M, Kurihara T, Sekiyama E, Maldonado AE, D'Amore PA. An essential role for RPE-derived soluble VEGF in the maintenance of the choriocapillaris. *Proc Natl Acad Sci USA* 2009; **106**: 18751–18756.
42 Fujita Y, Takeshita F, Mizutani T, Ohgi T, Kuwano K, Ochiya T. A novel platform to enable inhaled naked RNAi medicine for lung cancer. *Sci Rep* 2013; **3**: 3325.
43 Kariko K, Bhuyan P, Capodici J, Weissman D. Small interfering RNAs mediate sequence-independent gene suppression and induce immune activation by signaling through Toll-like receptor 3. *J Immunol* 2004; **172**: 6545–6549.
44 Lambert V, Lecomte J, Hansen S, Blacher S, Gonzalez ML, Struman I *et al.* Laser-induced choroidal neovascularization model to study age-related macular degeneration in mice. *Nat Protoc* 2013; **8**: 2197–2211.
45 Ishikawa K, Yoshida S, Kadota K, Nakamura T, Niiro H, Arakawa S *et al.* Gene expression profile of hyperoxic and hypoxic retinas in a mouse model of oxygen-induced retinopathy. *Invest Ophthalmol Vis Sci* 2010; **51**: 4307–4319.
46 Ishikawa K, Yoshida S, Nakao S, Sassa Y, Asato R, Kohno R *et al.* Bone marrow-derived monocyte lineage cells recruited by MIP-1beta promote physiological revascularization in mouse model of oxygen-induced retinopathy. *Lab Invest* 2012; **92**: 91–101.
47 Arima M, Yoshida S, Nakama T, Ishikawa K, Nakao S, Yoshimura T *et al.* Involvement of periostin in regression of hyaloidvascular system during ocular development. *Invest Ophthalmol Vis Sci* 2012; **53**: 6495–6503.
48 Yamaji Y, Yoshida S, Ishikawa K, Sengoku A, Sato K, Yoshida A *et al.* TEM7 (PLXDC1) in neovascular endothelial cells of fibrovascular membranes from patients with proliferative diabetic retinopathy. *Invest Ophthalmol Vis Sci* 2008; **49**: 3151–3157.
49 Lin H, Qian J, Castillo AC, Long B, Keyes KT, Chen G *et al.* Effect of miR-23 on oxidant-induced injury in human retinal pigment epithelial cells. *Invest Ophthalmol Vis Sci* 2011; **52**: 6308–6314.
50 Tanimoto N, Muehlfriedel RL, Fischer MD, Fahl E, Humphries P, Biel M *et al.* Vision tests in the mouse: functional phenotyping with electroretinography. *Front Biosci (Landmark Ed)* 2009; **14**: 2730–2737.